

Experimental investigation of forced convective heat transfer in cylindrical pipe flows

Yoshinori Hattori

Shibaura Institute of Technology, Mechanical Engineering

Tokyo, Japan

md18060@shibaura-it.ac.jp

I. INTRODUCTION

In recent years, forced convective heat transfer in cylindrical pipe flow has been playing an important role in many technical cooling systems. These coolant technology is used wide variety of coolant applications such as electric devices, automotive, and plant factory. Considering heat transfer issues, heat transfer coefficients are one of the most important numbers. The Nusselt number (Nu) is a dimensionless number which represents the ratio of convective (h) and conductive heat transfer (k), as expressed in Equation (1).

$$Nu = \frac{h \cdot L}{k} \quad (1)$$

For a general dimensional analysis, the Nusselt number represents function of the Reynolds number (Re) multiplied by the Prandtl number (Pr) as Equation (2).

$$Nu = \alpha \cdot Re^{\pi\beta} \cdot Pr^{\pi\gamma} \quad (2)$$

Here, factors α , β and γ are constant values that depend on flow regime.

In technology, flows regime and heat transfer plays an important role in considering engineering issues. Navie-Stokes equations describe the relation of variable flows. However, deterministic solution of the equations are only valid for small disturbances in the initial and boundary condition. In physically, it is hard to get initial and boundary conditions in infinite accurate. Turbulent has a large amount of fluctuations, i.e. turbulent is completely different kind of laminar flows. Direct Numerical Simulation (DNS) is one of the simulation way to predict flow forms. The object of the simulation is to solve the complete set of equation of motion without using any model. From Kolmogorov length scale, total number of computations is derived following equation (3). The DNS require large amount of total number of computations.

$$\mathcal{N} \times \mathcal{M} = \mathcal{O}(Re^{11/4}) \quad (3)$$

The equation implies the limitation of the DNS and that is directly connected to computer technology. Normally, engineers is interested in high Reynolds number such as aircraft or atmospheric boundary layer. However, such high Reynolds number requires huge amount of total number of computations and it's far from reality.

Therefore, it is necessary to get experimental data for correlations of heat transfer and flow condition and the Reynolds number.

Many studies have pointed out that a heat transfer coefficient varies depending on the type of flow: laminar, transition and turbulent. Gnienlinski [3] showed a calculation method about heat transfer coefficients for the laminar, transitional and turbulent flows. Bertsche et al. [4] focused on reliable prediction of the heat transfer coefficient for transitional flows. In their study, they showed experimental the heat transfer coefficients for the Reynolds number, $500 < Re < 23000$, and the Prandtl number, $7 < Pr < 41$.

However, not so many data is available for experimental data of laminar-to-turbulent transitional region. More studies should be conducted to obtain experimental data for high the Prandtl number and transitional flows. In this study, the author focused on forced convective heat transfer in flow of water and glycole in a cylindrical pipe. A 50/50vol% mixture of water and glycole, which is a typical liquid coolant in automotive applications, was used as an operating fluid. The experiment was carried out by considering a board range of Reynolds numbers, spanning from a laminar to fully turbulent flow. Moreover, the measurements of the wall friction coefficients was also performed in this study.

II. EMPIRICAL CORRELATIONS

A. The friction coefficients

The skin friction coefficients for laminar flow is described following equation.

$$C_{f,lam} = \frac{16}{Re_b} \quad (4)$$

Konakov [2] showed the skin friction coefficients for turbulent flow.

$$C_{f,turb} = 0.25(1.8\log(Re_b) - 1.5)^{-2} \quad (5)$$

B. The heat transfer coefficients

Gunienski [3] showed correlations for each flow conditions: laminar, transitional and turbulent, respectively. Gunienski [3] showed calculation method for laminar flow.

$$Nu_{lam} = (3.66^3 + 0.7^3 + (1.615(Re_b Pr_b \frac{d_i}{L})^{1/3})^3)^{1/3} \quad (6)$$

He showed calculation method for turbulent flow.

$$Nu_{turb} = \frac{\frac{C_{f,turb}}{2Re \cdot Pr_b}}{1 + 12.7 \sqrt{\frac{C_{f,turb}}{2}} (Pr_b^{2/3} - 1)} \cdot \left(\frac{Pr_b}{Pr_w}\right)^{0.11} \quad (7)$$

The range is

$$0.1 \ll Pr_b \ll 1000, 10^4 \ll Re_b \ll 10^6 \quad (8)$$

He presented transitional flow as a liner interpolation between turbulent and laminar flow.

$$Nu_m = (1 - r)Nu_{m,lam} + rNu_{m,turb} \quad (9)$$

$$r = \frac{Re_b - 2300}{10^4 - 2300} \quad (10)$$

III. EXPERIMENTAL SETUP

Figure. 1 shows a diagram of the experimental loop. The experimental basically loop consists of a heat exchanger, a pump, a Coriolis mass flow rate, a welder, a reservoir, and a test section. The heat exchanger keeps a thermal stationary condition in the flow pipe. The Coriolis mass flow rate is controlled by the pump and a bypass valve C, which is located in parallel to the pump. The pipe is thermally insulated by using glass wool.

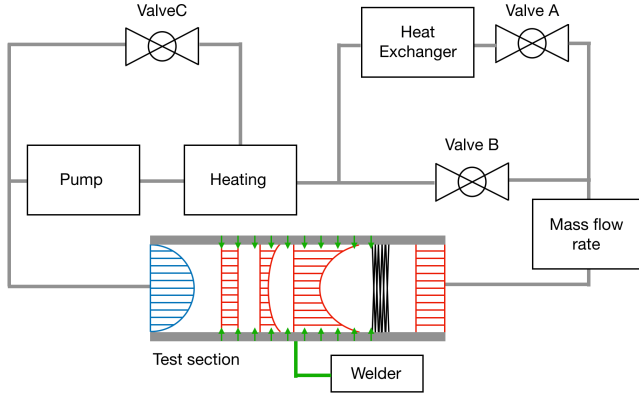


Fig. 1. Process flow diagram of the test facilities including test section.

Figure. 2 shows the velocity and thermal boundary layer developments vary with the horizontal axis in the test section. The velocity and thermal profiles are shown in blue and red color, respectively. The test section is made of stainless steel (1.4301) with an inner diameter $d_i=12\text{mm}$ and outer diameter $d_o=15\text{mm}$. Highly accurate resistance thermall probes (PT-100) are used to find out the inlet and outlet bulk temperatures (T_{b0} , T_{b1}) and wall temperature (T_w). Moreover, thermocouples (Type-K) are used to measure temperature gradients in the flow direction.

The test section consists of entrance, heated and thermal equalized parts.

1) Entrance part

The first part of the test section is a 1.2 [m] length entrance part, which is sufficiently long to ensure producing dynamically developed flow condition at the

exist. The bulk temperature (T_{b0}) at this section was measured by PT-100.

2) Heated part

The second part of the test section is a 2 [m] length heated part, which is sufficiently long to ensure producing thermal fully developed flow condition at the exist. The tube wall were heated electrically by the welder which provides high current and low voltages to keep the uniform heat flux condition in a inner pipe flow. Convective heat transfer is independent of the horizontal axis in fully developed flow and constant heat flux condition. The wall temperature (T_w) at the end of this section were measured by PT-100.

3) Thermal equalized part

The third part of the test section is the thermall equalized part, which includes a Static mixture. The static mixture forms turbulent and vortex. Then, the thermal gradients of fluids become averaged, and bull temperature (T_{b1}) is measured.

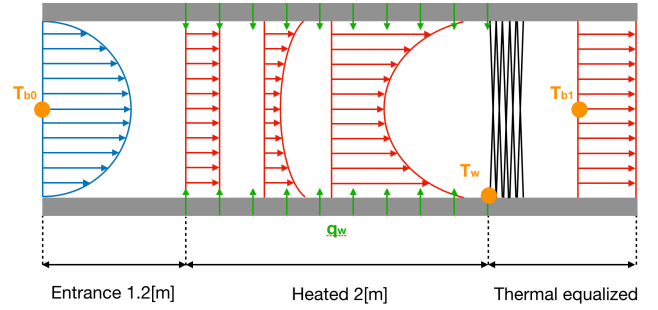


Fig. 2. Velocity (blue) and thermal (red) boundary layer development vary with horizontal axis in a test section.

A. Length-to-diameter ratio

The length-to-diameter ratio is an important parameter to achieve the fully developed turbulent condition in the test section. The entrance section has an inner diameter of $d_i = 12\text{mm}$, and the length of $L = 1.2\text{m}$ which length-to-diameter ratio is $L/d_i = 100$. Patel et.al. [1] showed suitable the length-to-diameter ratio for fully developed turbulent flows. According to their study, they found that the minimum developing length of $L/d_i = 70d_i$. Therefore, the length-to-diameter ratio of the entrance section in this experimental is long enough to ensure the fully developed turbulent flow state.

B. Wall roughness

To clarify the wall surface as a smooth pipe, wall roughness was considered. Moody diagram defined the basis of friction chart, and that can be used in practice. Nikuradse made a throughout studies of turbulent flows in pipes with a rough surface. Reynold number can be interpreted as the ratio between the rough height h and thickness of the viscous sublayer ν/u_* , as the following equation.

$$Re = \frac{hu_*}{\nu} \quad (11)$$

Here, u_* represents wall friction velocity and described following equation.

$$u_* = \sqrt{\frac{\tau_{wall}}{\rho_0}} \quad (12)$$

Wall roughness of a characteristic height is described following equation.

$$h = 4k_{rms} \quad (13)$$

In this experiment, the surface roughness of interior surfaces in stainless steel (1.4301) is approximately $k_{rms} = 5\mu m$. Table I shows roughness consideration in this experiment. It is

TABLE I
ORDERS OF EACH TERMS IN EQUATION

surface roughness	roughness height	viscous sublayer	Re
$5\mu m$	$20\mu m$	$0.4\mu m$	0.48

shown that the Reynolds number in this experiment is less than 1. Thus, the interior wall surface in the experimental setup is considered to be a smooth surface.

C. Velocity profiles

Turbulent velocity profiles for the smooth wall as following equation.

$$\bar{u} = u_* \left[\frac{1}{k} \ln \left(\frac{y}{h} \right) + B' \right] \quad (14)$$

B' is a function of the Reynolds number and calculated as following equation.

$$B' = 2.5 \ln \left(\frac{hu_*}{\nu} \right) + 5 \quad (15)$$

Figure 3 shows mean velocity profile when $Re = 2300$ and $Pr = 50$.

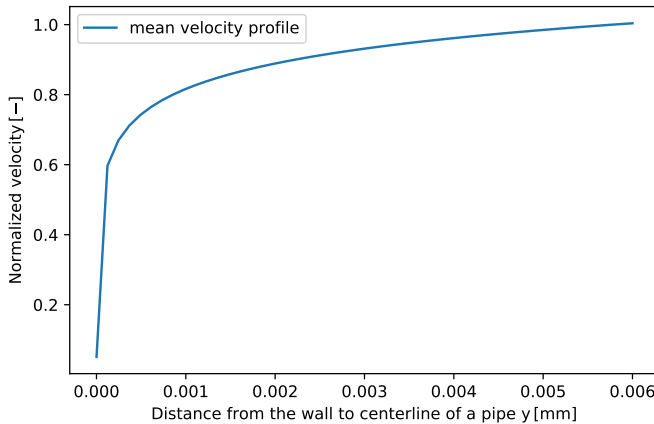


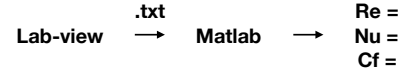
Fig. 3. mean velocity profile when $Re=2300$ and $Pr=50$.

IV. EFFECTIVE DATA PROCEDURE

V. CALUCURATION FLOW

Since all materials can be expressed by temperature-dependent functions. At first, the author measured the material properties of density ρ , heat conductivity k , specific heat transfer Cp , kinetic viscosity ν , dynamic viscosity μ , Prandtl number Pr that depend on temperature. Next, he measured temperature differences, pressure differences and mass flow rates of the test section. Finally, Nusselt, Prandtl, Reynolds numbers and friction coefficients were calculated by post-processing with LabView and MATLAB. Figure 4 shows developed improvement post-processing compared compared with 2018. In 2018, the author needed to take the result from Matlab file by file. It takes long time to deal with many data efficiently. Thus, he developed a new Python code which can calculate Reynolds number, Nusselt number and friction coefficients, and plot those numbers automatically.

2018



2019: Automated

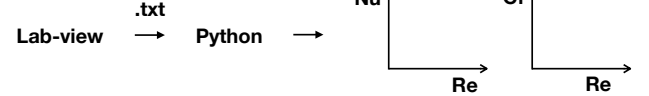


Fig. 4. Developed improvement post processing compared with 2018

VI. RESULTS AND DISCUSSIONS

Data obtained in previous study [5] using the same experimental facilities indicated that heat transfer and friction coefficients for Shell Heat Transfer Oil. The aim of this research is to investigate heat transfer and friction coefficients using water-glycol 50%/50% mixture as an operating liquid. In order to investigate Prandtl number thoroughly, first the experimental results for $Pr=50$ is compared with data obtained in previous studies [5] using Shell Heat Transfer Oil for Prandtl numbers $Pr=50$. Therefore, the validity of evaluation process for the experiment are checked.

Figure. 5 shows dimensionless heat transfer coefficients for $Pr = 50$ compared to empirical correlations equations (6)(7)(9) and previous studies.

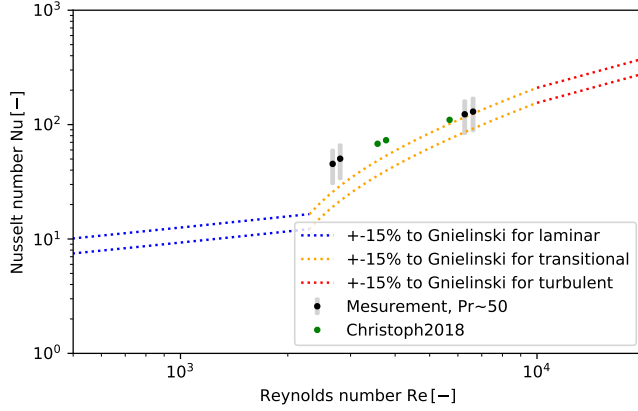


Fig. 5. Dimensionless heat transfer coefficients compared to literature data and previous studies for $Pr = 50$. The red, yellow and blue lines are Gnielinski correlations for laminar, transitional and turbulent, respectively.

Figure. 6 shows friction coefficients compared to empirical correlations equations(4)(5) and previous studies. As can be seen,

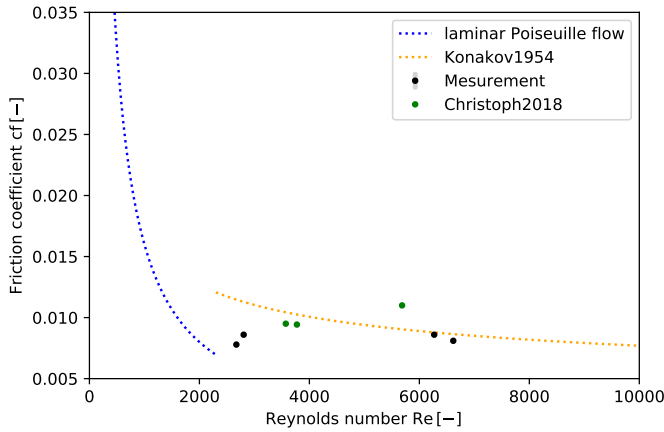


Fig. 6. Friction coefficients compared to literature data for $Pr = 50$. The red and blue lines are empirical correlations for laminar and turbulent flows, respectively.

seen, it is obvious that the experimental results on friction coefficient for $2200 < Re < 7000$ are very well fitted by the cited correlations, which is consistent with results obtained in previous studies. However, the data for heat transfer were not consistent with these result for transitional flow regime. Although heat transfer for higher-transitional flow regime were in line with those of Gnielinski [3] correlations, a striking difference was noted for lower-transitional flow regime. Since all material properties can be expressed by temperature-dependent functions, it is difficult to keep a high Prandtl number and a transitional Reynolds number. For example, as enhance cooling, static viscosity increase. As a result, the Prandtl number increase and the Reynolds number decrease.

Those numbers are related. In correlations, the Prandtl number was assumed to be constant value. However, the experimental Prandtl number was not constant because the fluid properties vary with temperature. In this study, the author tried to keep the Prandtl number constant but it was not achieved. Thus, he plot the heat transfer and the Reynolds number for the Prandtl number as devide some cases.

A quantitative analysis to determine measurement uncertainties was applied, based on estimating the maximum possible error in the parameters evaluated from measurement data. The uncertainty of measurement was analyzed by using “Guide to the Expression of Uncertainty in Measurement”(GUM). Nusselt number is calculated from Equation (16).

$$Nu = \frac{\dot{m}c_p(T_1 - T_0)}{\lambda(T_w - T_1)d\pi L} \quad (16)$$

The uncertainty in Nusselt number is calculated from Equation (17).

$$Nu = \sqrt{\sum \left(\frac{\partial Nu}{\partial X_i} \Delta X_i \right)^2} \quad (17)$$

Each parameter, X effects each parameters of Equation (16). Then, the measurement uncertainty in Nusselt number leads to Equation (18).

$$\begin{aligned} \frac{\Delta Nu}{Nu} = & \sqrt{\left(\frac{\Delta \dot{m}}{\dot{m}} \right)^2 + \left(\frac{\Delta c_p}{c_p} \right)^2 + \left(\frac{\Delta \lambda}{\lambda} \right)^2} \\ & + \left(\frac{\Delta T}{T_0 - T_1} \right)^2 + \left(\frac{\Delta T(T_0 - T_w)}{(T_0 - T_1)(T_1 - T_w)} \right)^2 + \left(\frac{\Delta T}{T_1 - T_w} \right)^2 \end{aligned} \quad (18)$$

The measurement uncertainty in friction coefficients leads to Equation (19)

$$\frac{\Delta C_f}{C_f} = \sqrt{\left(\frac{\Delta P}{P} \right)^2 + \left(\frac{\Delta \rho}{\rho} \right)^2 + 2 \left(\frac{\Delta \dot{m}}{\dot{m}} \right)^2} \quad (19)$$

Based on this approach, the average uncertainty of the measurement for this study were shown in previous. Table (II) shows the orders of each terms in Equation 18. From this comprehensive result, temperature term is several orders of magnitude larger than others. Therefore, temperature measurement is strongly inflected to measurement uncertainty. According to this analysis, careful selections of temperature sensors are needed.

TABLE II
ODERS OF EACH TERMS IN EQUATION 18.

	Mass flow	Specific heat capacity	lambda	Temperature
Order	O (-8)	O(-8)	O(-8)	O(-4)

VII. FUTURE PLAN

An operating fluid was changed from Shell Heat Transfer to Water-glycol. And new accurate thermocouples were replaced. The author describes future plans below.

- 1) Modify Labview program for the new thermocouples
- 2) Take material properties for water-glycole
- 3) Check validity of the result with Bertsche et al. [4]. They showed heat transfer coefficients for $500 < Re < 23000$ and $7 < Pr < 41$ for water glycol mixture
- 4) Focus on transitional and high Prandtl number
- 5) Compare with already existing numerical simulations (CFD) and empirical correlations
- 6) Documentation

VIII. APPENDIX

The experiment was carried out already existing facilities by Christphan 2018 [5]. Experimental procedure is as follows.

- 1) Switch on (Ein) Main switch (S0)
- 2) Start up a computer
 - a) Select "Rohr.lvproj"
 - b) Select Lab VIEW and click "Starten"
 - c) Click "Nein"
 - d) Select "Rohrpufsp.vi"
- 3) Prepare water supply for cooling experimental facilities.
 - a) Open the tap water and save cool water in big tank.
 - b) Check the temperature is approximately 15°C .
 - c) Check the valves are in following state. Valve A is closed, B is opened, and C is closed.
 - d) Turn on pump switch to supply cooling water
- 4) Check the value of mass flow rate on PC display and wait until the value is approximately 0.
- 5) Click T_s allec and T_s gleci to carry out Temperature calibration
- 6) Switch on heater (S1: Heizstab)
- 7) Click "Aushmine" to start the experiment
- 8) Set "Welder stom" under 300A
- 9) Switch on the pump (S4: Pump)
- 10) Switch on the welder
- 11) Adjust suitable experimental parameters for Re and Pr.
 - a) Decrease Re and increase Pr
Open valve A and close valve B little by little. As enhance cooling, static viscosity increase.
 - b) Decrease Re and decrease Pr
 - c) Decrease Re and keeps Pr constant
- 12) Wait until the condition reaches steady
- 13) Click "Schreiben" to save the data
- 14) Switch of the Welder
- 15) Open the valves (flow max) and cool down the facilities
- 16) Wait until the facilities cool down enough
- 17) Turn off pump switch to stop supplying cooling water
- 18) Switch off the pump (S4: Pump)
- 19) Close the tap water
- 20) Click "close" for LabView application
- 21) Shut down PC and click "Klick sie heir unclear—", not to download any current version

REFERENCES

- [1] Zanon, E.-S., M. Kito and Ch. Egbers, "A study on Flow Transition and Development in Circular and Rectangular Ducts." Journal of Fluids Engineering, 131(6)-061204.
- [2] Konakov, P. K., "Eine neue Formel fr den Reibungskoeffizienten glatter Rohre", 1954, Bericht der Akademie der Wissenschaften der UDSSR 51.7, 503–506.
- [3] V. Gnienlinski, "Heat Transfer in Laminar Flow," VDI Heat Atlas, second ed., Springer Verlag, 2010 (Chapter Ga 1-7), Section 3.
- [4] Dirk Bertsche, Paul Knipper, Thomas Wetzel, "Experimental investigation on heat transfer in laminar, transitional and turbulent circular pipe flow," International Journal of Heat Transfer, 95 (2016) 1008-1018.
- [5] Christphan, "Title of paper if known," unpublished, 2018.
- [6] Emir Öngüner, 'Experiments in Pipe Flows at Transitional and Very High Reynolds Numbers', Cuvillier Verlag, 2018.
- [7] Frans T.M. Nieuwstadt, Bendiks J. Boersma and Jerry Westerweel, "Turbulence: Introduction to Theory and Applications of Turbulent Flows", (Springer, 2016)3-4, 71-74, 101-102, 176-181.
- [8] Frank P. Incropera et al., "Fundamentals of Heat and Mass Transfer", (Wiley, 2006)